

Strategy for Dynamic Wisp Removal in James Webb Space Telescope NIRCам Images

A. S. G. Robotham,^{1,2} J. C. J. D’Silva,^{1,2} R. A. Windhorst,³
R. A. Jansen,³ J. Summers,³ S. P. Driver,¹
C. N. A. Wilmer,⁴ S. Bellstedt,^{1,2}

¹ICRAR, M468, University of Western Australia, Crawley, WA 6009, Australia

²ARC Centre of Excellence for Astrophysics in Three Dimensions (ASTRO3D)

³School of Earth and Space Exploration, Arizona State University, Tempe, AZ 85287-1404, USA

⁴Steward Observatory, University of Arizona, 933 N. Cherry Avenue, Tucson, AZ 85721-0009, USA

Exact ordering to be determined (above I am adding people as they respond).

E-mail: aaron.robatham@uwa.edu.au

April 2023

Abstract. The James Webb Space Telescope (JWST) near-infrared camera (NIRCам) has been found to exhibit serious wisp-like structures in four of its eight short-wavelength detectors. The exact structure and strength of these wisps is highly variable with the position and orientation of JWST, so the use of static templates is non-optimal. Here we investigate a dynamic strategy to mitigate these wisps using long-wavelength reference images. Based on a suite of experiments where we embed a worst-case scenario median-stacked wisp into wisp-free images, we define suitable parameters for our wisp removal strategy. Using this setup we re-process wisp-affected public Prime Extragalactic Areas for Reionization and Lensing Science (PEARLS) data in the North Ecliptic Pole Time Domain Field (NEP-TDF) field, resulting in significant visual improvement in our detector frames and reduced noise in the final stacked images.

1. Introduction

The James Webb Space Telescope (JWST) is a truly exceptional near- and mid-infrared facility [1], with multiple major surveys being conducted and proposed using its wide-field near-infrared instrument NIRCам [2, 3, 4]. Not unusually for a new facility, various facets of the data are slowly being understood and their calibration and mitigation improved by the astronomical community, e.g. image persistence, cosmic rays and snowballs. One of the most difficult to detect and correct are ‘wisps’. Wisps are present

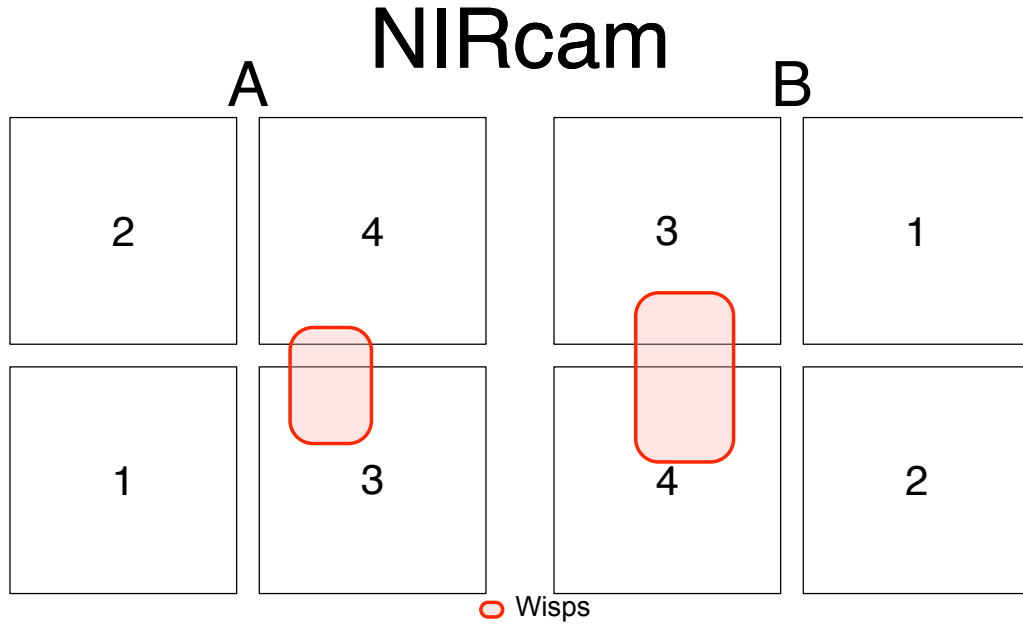


Figure 1. Schematic layout of NIRCam short wavelength modules (A and B) and their individually numbered detectors (1–4). The intra- and inter-module gaps are not to exact scale. Wisps are most visually prevalent in detectors A3, A4 and B3 and B4 (i.e. the central detectors), as indicated by the red regions.

as cloud-like cirrus features on certain combinations of NIRCam filters and detectors[‡]. For reference, Figure 1 shows the approximate layout of the NIRCam short-wavelength modules and detectors (where wisps are prevalent).

Wisps appear to have a scattered-light origin, predominantly due to off-axis light from bright stars hitting the top secondary mirror strut and entering NIRCam through the aft-optic system. The STSci web pages suggest that the wisps should only really vary in strength for a given filter-detector combination, however experience with Prime Extragalactic Areas for Reionization and Lensing Science [PEARLS; 2] data reveals that wisp intensity and geometry can change quite significantly even for small (hundreds of pixel) dither offsets of a given filter-detector combination. This makes constructing static templates a potential dead-end for robust frame level removal as they are strongly sensitive to the exact geometry, intensity, and spectrum of off-axis light.

Wisps only appear in the short-wavelength detectors of NIRCam and are most visually prevalent in module A detector 3 (top-left quadrant of the frame) and detector 4 (bottom-left quadrant of the frame), and module B detector 3 (bottom-middle of the frame) and detector 4 (top-middle of the frame). The wisp-affected data correspond to the middle four detectors in Figure 2. Module B detector 4 has by far the most

[‡] <https://jwst-docs.stsci.edu/jwst-near-infrared-camera/nircam-features-and-caveats/nircam-claws-and-wisps>

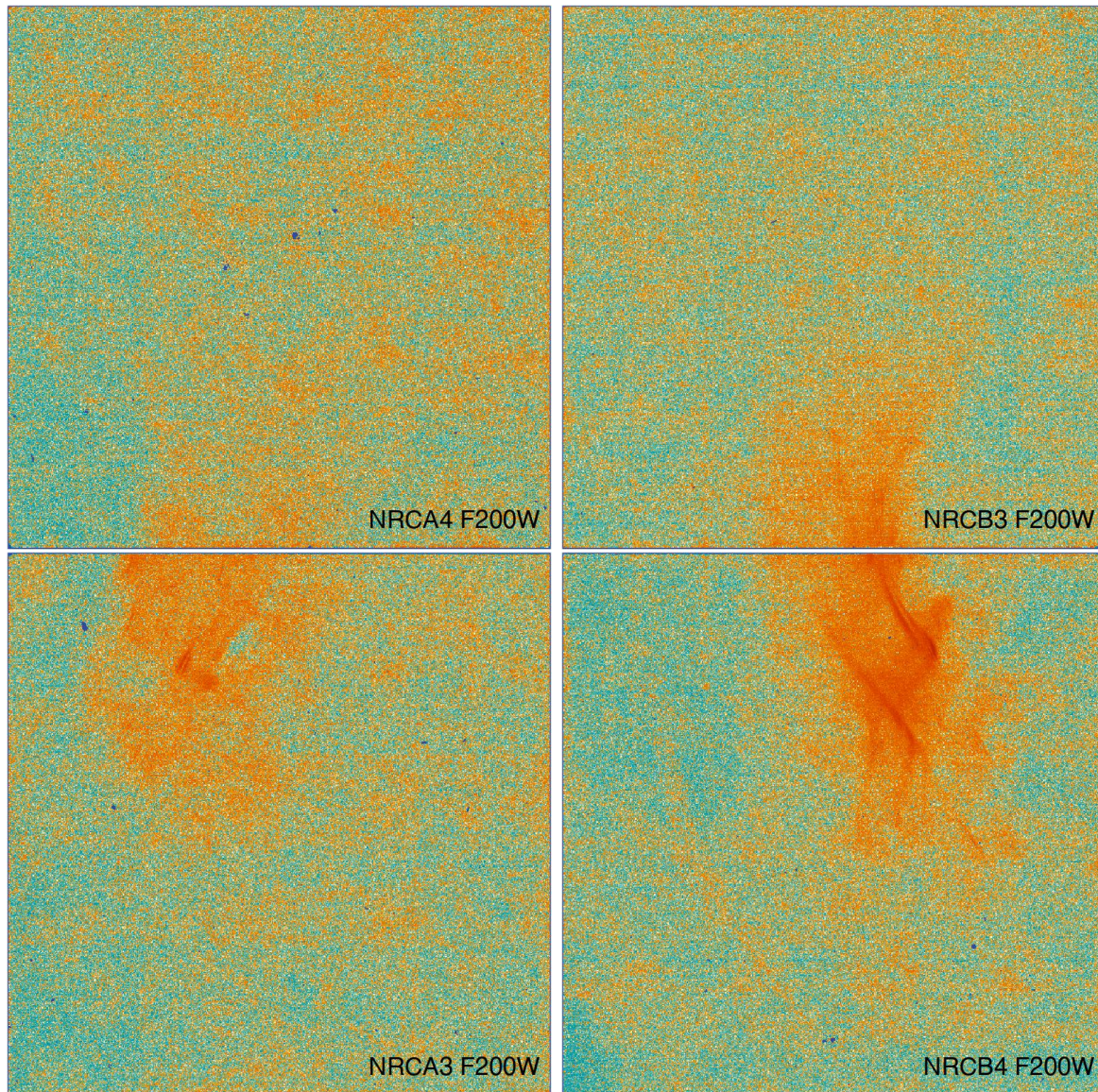


Figure 2. STSci wisp templates created for module A detector 4 (top-left) and detector 3 (bottom-left); and module B detector 3 (top-right) and module 4 (bottom-right). The layout is chosen because it approximately reflects the true detector layout geometry of NIRCam (see the middle frames of Figure 1, and wisp regions highlighted). Each image is median-subtracted and displayed with a blue-yellow-red asinh ramp (blue showing below-median pixels and red above-median pixels), with the wisps being the prominent central red features crossing module A filters 3–4 and and module B filters 3–4. Whilst NRCB4 shows the most dramatic wisp structure, even NRCA4 has enough wisp strength to create artifacts in large stacks of images with small dithers.

dramatic wisps when present, where the embedded filamentary features can sometimes achieve galaxy-like surface brightnesses. In general the F200W filter has the most serious artifacts from wisps, followed by F150W and often (to a much lesser extent) F115W and F090W. The fact that the geometry of the wisp varies so much with wavelength explains

why the wisps vary even in a given filter. Clearly the spectrum of the off-axis nuisance source changes the integrated wisp pattern even within a filter. We note that STSci has only created wisp templates for filters F150W, F200W and F210M (created by CW using commissioning plus public data up to late August 2022), so F115W and F090W in particular need a remedial strategy despite cases where the other filter templates appear to work well at mitigating the wisps. Even where STSci templates are available, there are quite a few artifacts (hot and cold pixels) and low signal-to-noise in much of the frame.

Given the above statements it is intuitively clear that some programs and visits will have fewer wisp issues (due to the good fortune of exactly where off-axis sources happen to lie), and others might be seriously compromised. In the PEARLS medium-deep survey fields there are examples of detector-filter combinations with no visual wisps apparent in our final stacks, and other cases where wisps are highly prominent and problematic for further analysis. This paper will investigate dynamic strategies for optimally removing wisps. We believe these approaches will prove useful to the broader community for any and all future medium and deep surveys with NIRCam in order to achieve \sqrt{T} improvements in depth with increasing exposure time (T) across all NIRCam filters.

2. Wisp Removal

Having identified wisp residuals in inverse-variance-weighted and median stacks of PEARLS fields, it became clear that better dynamic strategies were necessary for us to extract maximum science from the observations. This was particularly true of the PEARLS Northern Ecliptic Pole Time Domain Field (NEP-TDF, often referred to as just NEP or TDF in PEARLS related literature) field, which due to unfortunate coincidence tends to be particularly affected by wisps. Given it will be one of the deeper wide JWST fields, it is paramount we mitigate their presence as much as possible.

First efforts in this direction relied on the automated sky detection capabilities of PROFOUND as detailed in [5, 6] and [2]. This worked well for some filter-detector-field combinations, where the wisp happened to have a quite smooth and extended characteristics. The best metric of quality in these scenarios is the Normality of the nominal sky background pixels, since a well-characterised sky (both in terms of background and root-mean-squared (RMS) deviation) should have a mean of zero and a standard deviation of one. It was clear though that some particular filter-detector-field combinations had features not captured by the smooth sky modelling assumptions that underly PROFOUND's background subtraction methods. Most seriously, bright streaks in module B detector 4 have a far too high spatial frequency to be modelled as sky without creating serious self-subtraction issues.

2.1. Colour Difference Flagging

When analysing large quantities of stacked and mosaicked NIRCam data, a consistent finding was that wisps, whilst present to varying degrees in all of the short-wavelength detector combinations, are *never* present in the long-wavelength detectors (F250M and long-wards). The wisp feature and behaviour with wavelength was also noted in [7]. This offers a conceptual solution to identifying wisps in a dynamic manner: if features are only present in a short-filter frame compared to a reference long-filter stacked image of similar or greater depth, then it is likely the feature is a scattered light wisp rather than an extremely blue object.

After some experimentation with a variety of methods, the following strategy produces consistent good quality (low residual) stacked data:

- (i) project a long-wavelength filter (cosmetically F444W is often best, but F356W works similarly well) stacked mosaic to match the world coordinate system (WCS) of a target short-wavelength filter frame that has wisps to be removed;
- (ii) calculate the most extreme plausible blue colour (B_{lim}) that you might expect between the short and long filters (this could be computed theoretically from e.g. the spectrum of O stars, or estimated dynamically from the images being processed);
- (iii) for pixels bluer than this limit create a map of the flux differences (this is the initial wisp template, WT);
- (iv) smooth the WT with some kernel that is smaller than the highest frequency wisp, but large enough to overcome Poisson photon noise in the map;
- (v) set to zero pixels in the WT that are above some threshold (this avoids bright pixels around stars being flagged as wisp features purely due to wavelength-dependent differences in point spread functions (PSFs));
- (vi) subtract the final WT map from the target frame to be corrected.

We find that dynamically calculating the bluest plausible colours (B_{lim}) based on image statistics works well in practice, and lends the technique greater flexibility when using different combinations of short- and long-wavelength filters. There are a number of ways to achieve this reasonably, but our preferred strategy is:

- (i) create a map of WCS-matched relative fluxes (RF) between the short-filter image to be fixed (numerator) and long-wavelength stacked reference image (denominator);
- (ii) select pixels in RF corresponding to the brightest 10% of pixels in the long-wavelength stacked WCS-matched reference image (these pixels are highly likely to belong to real sources given the depth of PEARLS and similar imaging data);
- (iii) remove any negative-valued pixels (there should not be many, but we only want to analyse positive-ratio pixels);
- (iv) compute the 95th percentile of the remaining RF pixels (ranked low to high), and treat this as the bluest plausible value (B_{lim}) for future analysis (this is the main

parameter that controls how aggressively sources are masked out, higher meaning more masking).

The main parameters discussed above were chosen based on visual inspection of wisp-removed frames and the results of mock wisp-removal simulations (discussed in more detail later in Section 2.2). The quality of wisp removal is not highly sensitive to the exact values chosen. For the source threshold, values between 1–20% of brightest pixels work well (we default to 5%). For defining blue colours, values between 80–99% work well (we default to 95%). For final clipping, values between 99–100% work well (we default to 99.7%). The optimal smoothing is more subjective, but for PEARLS-depth data, setting the standard deviation of a Gaussian smoothing kernel to 2 pixels appears to be a good compromise of resolution and signal, but values between 0.5 and 3 pixels work well.

We also investigated the best strategy for defining wisp templates in the regions where we have masked objects. In general, the complex structure of the wisps cannot be well approximated by interpolating through large regions of missing pixels. Early tests also showed that various methods (bicubic or bilinear spline interpolations, kernel smoothing, and polynomial regression) could all produce pathologically bad results for pixels far from real data. In most cases, the wisps lying under a source are much lower surface brightness than the source, and ignoring wisps in these areas does little harm (and is our preferred method). Note, the main aim for removing wisps is to produce better (flatter) backgrounds for later removal, and also to remove completely spurious sources produced by wisps. For sensibly dithered data (at the scale of the wisps) clipping and/or median stacking should further mitigate small residual wisp signal lying within sources.

2.2. *Calibrating and Testing*

It is important to test and calibrate the aggressiveness of any wisp removal scheme, since we do not want to remove real flux from the image or (ideally) leave any wisp flux behind. To optimise our wisp removal parameters we used a median-stack wisp template for filter F200W and detector NRCB4 (detector 4 of module B) since this is generally the worst wisp-affected filter-detector combination (see Figure 4). We then embedded this wisp template in 64 NRCA1, NRCA2, NRCB1 and NRCB2 frames (which are visually wisp-free) and attempted to remove the wisp with our automated scheme outlined above.

Depending on the frame (and the fluxes of the real sources) the added wisp contains in the region of 10-20% of the total pedestal subtracted flux in the image. It is often the brightest single ‘object’ in the image, but since it is distributed over a large area it is usually also the lowest average surface brightness structure. These properties give some sense of the significance of wisps in terms of how much they can compromise JWST data, and also why removing them is a challenging task.

The default values presented above allow for nearly optimal wisp removal, where we err on the slightly aggressive side since local regions of over-subtraction are more easily

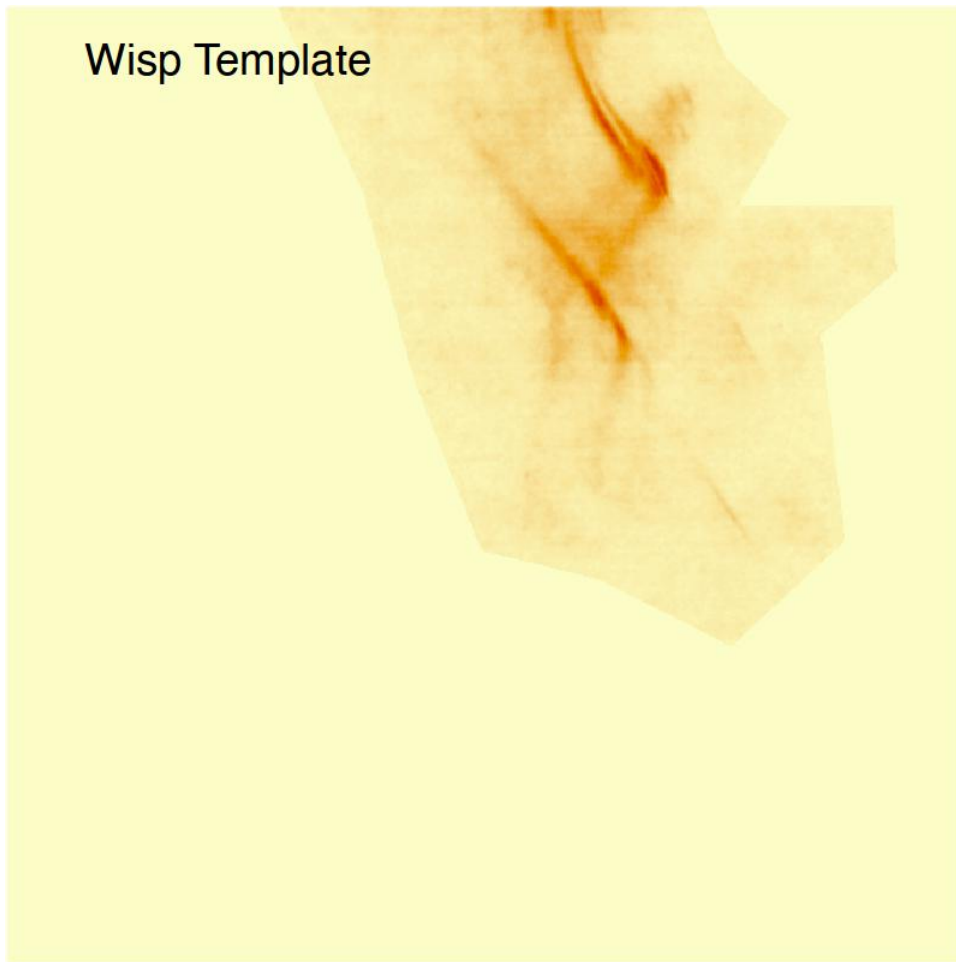


Figure 3. Example of a simulated wisp template for a F200W filter frame and detector NRCB4 (detector 4 of module B). This is a masked, pixel-clipped and slightly smoothed (to reduce pixel noise) version of the bottom right panel of Figure 2 using the wisp templates made available at STSci (linked above). Colour scaling is per Figure 2.

fixed during later image stacking (the worst over-subtractions happen near bright stars where pixels will be flagged). Figure 4 shows an example of a frame where the embedded wisp has been cleanly removed, and the final wisp template generated is visually close to the unknown (to the algorithm) wisp template embedded. The highest-resolution features of the embedded wisp cannot be fully recovered due to the lower signal-to-noise of the real data in a single frame.

Overall the parameters discussed above work well for JWST NIRC*am* data, with on average 88.1% (mean) of the wisp template flux accounted for during this automatic modelling process. Figure 5 presents the overall statistics for 64 simulated wisp frames. We find that whilst we do not, on average, perfectly remove the embedded wisps, our processing technique always improves the flux measurements (all values are bounded between -1 and +1), i.e. we do more good than harm in all situations. Since the higher surface brightness parts of the wisp are usually very well removed, the remaining features

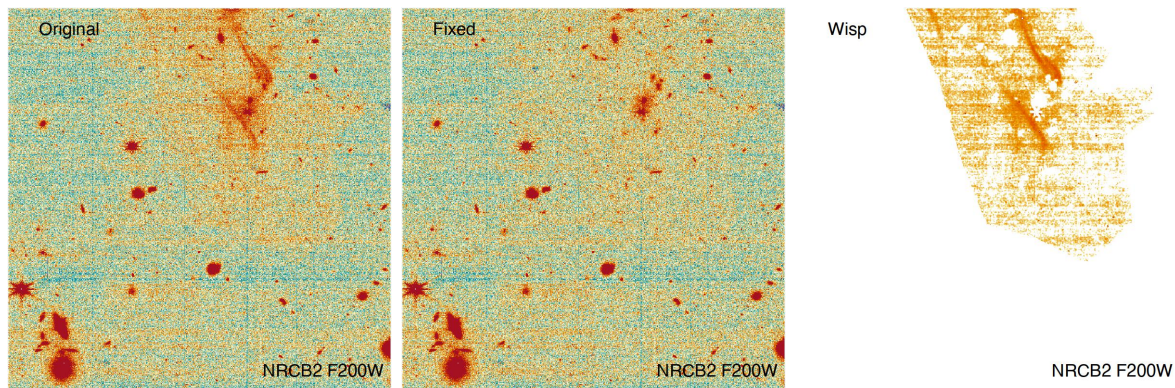


Figure 4. Example of simulated wisp removal. The wisp template shown in Figure 3 is embedded into the image at the level seen for particularly bad wisps. The image on the left is a F200W filter frame from NRCB2 (detector 2 of module B) taken as part of PID 2738 (VID 2738002001). The original image was visually free of wisps before the template was added. The centre image shows the result of the wisp subtraction method, where the cloudy structure at the top middle of the left panel has largely been removed. The right hand image shows the wisp template that was subtracted (white pixels are the fully masked regions of the wisp that correspond to pixels we do not want to modify). Colour scaling is per Figure 2.

(be they slightly positive or negative) are much smoother and easier to remove at later stages of the PEARLS processing pipeline. In particular the $1/f$ and PROFOUND sky subtraction stages work together to flatten out the remaining residuals in most situations.

2.3. Achieving \sqrt{T} Stacking

As a final test, a comparison was made of images stacked using PROPANE[§]. The wisp-free stack of F200W data was compared to the wisp-added stack (using the mock template above), and then the wisp-added and corrected stack (‘wisp-fixed’, using the approach discussed in this work). In this test all frames had the same exposure time (419s), so \sqrt{T} depth improvement is equivalent to a \sqrt{T} improvement. For the NEPTDF data used for the template simulations above, the deepest regions of our stack combine as many as eight individual frames (10.7% of the total area), and due to the masking and dithering strategy used there are many pixels with only one contributing frame (1.6%). At nominal depth (most of the area), four frames contribute to the stack.

To test the impact of stacking, we first create a deep segmentation map using the cosmetically clean F444W data warped (reprojected and resampled) with PROPANE to the same WCS as our target stack. To do this we use PROFOUND with default settings [for details see 5]. The non-object pixels identified during this process can then be used to measure background statistics, and to confirm whether we are able to achieve \sqrt{T} noise reduction with our wisp removal strategy.

[§] <https://github.com/asgr/ProPane>

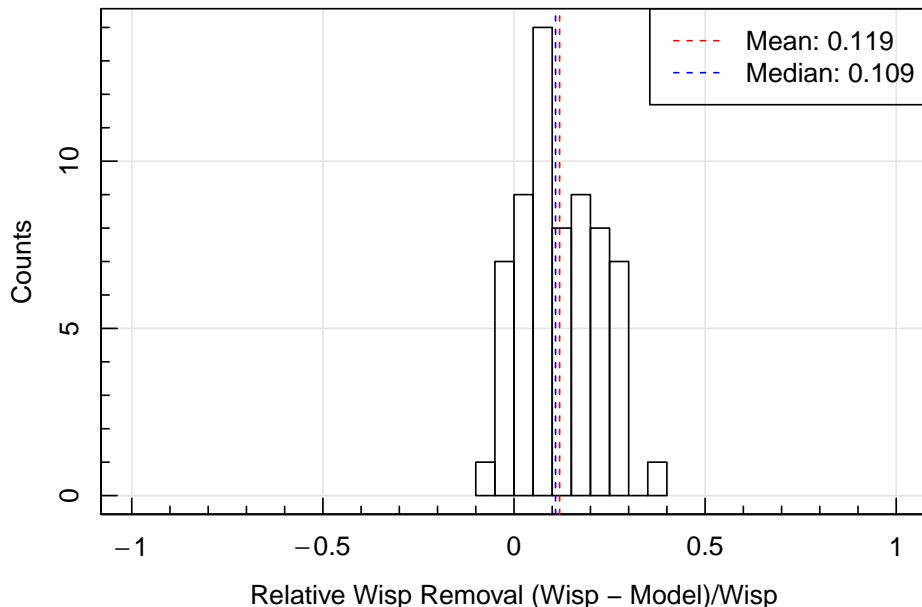


Figure 5. Relative wisp residual statistics. Negative values indicate frames where our wisp removal method has over-subtracted compared to the original embedded wisp template, and positive values indicate where we have under-subtracted. The mean and median statistic suggests a small degree of systematic over-subtraction on average (close to 0). The maximum over-subtraction is less than 10% of the wisp signal, and the maximum under-subtraction is less than 40% of the wisp signal (i.e. we err on the side of not being too aggressive with our removal process).

Firstly, we find that using the wisp-free data we achieve close to a \sqrt{T} increase in image depth (reduction in background root-mean-square noise; or RMS). More precisely, we find our image depth increases as $\frac{\sqrt{T}}{1.012^T}$. The slight deviance from perfect \sqrt{T} noise reduction is mostly due to covariance created during stacking (which will always be present when combining non pixel-aligned data) and the presence of non-detected sources in the ‘background’. Also, absolute read-noise levels will prevent \sqrt{T} noise reduction. This analysis is used as our best-case-scenario reference measurement for wisp removal.

We then compare the background RMS using the wisp-added data, and then finally the wisp-fixed data. The stacked images for all three scenarios are shown in Figure 6. When measuring the background statistics of the wisp-added data we find an RMS that is a factor 1.460 larger over the whole stacked frame (for pixels with eight frames contributing, our maximum depth). This is akin to saying we reduce the exposure time by a factor 2.4. When applying our wisp-removal strategy we obtain a background RMS that is a factor 1.026 larger over the same pixels, which is an effective reduction in exposure time of only a factor 1.05. Using the above slight non-linearity with \sqrt{T} , we find that we measure an RMS of our deepest pixels (eight frames contributing) a factor 1.10 larger than the $\sqrt{8}$ reduction we could expect with no data limitations. This

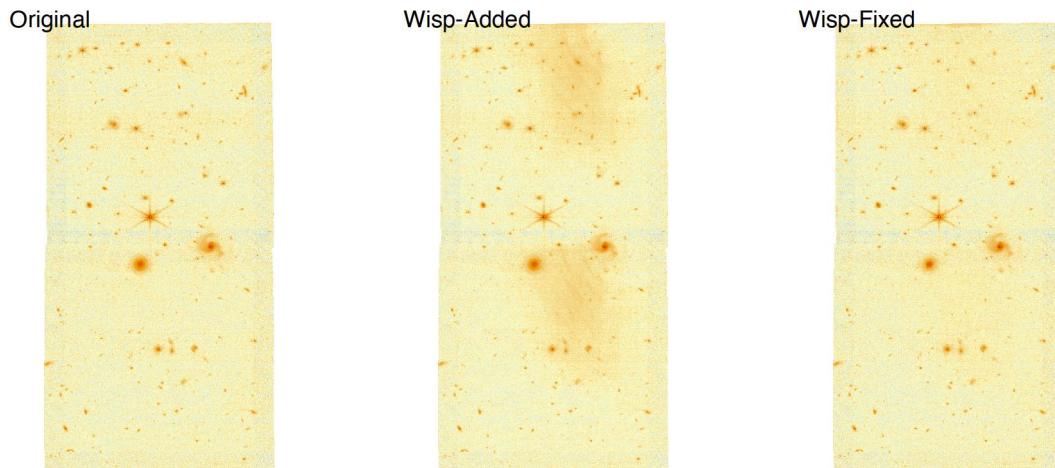


Figure 6. Example of simulated wisp stacking. The left panel shows a stack of 16 frames (with maximally eight frames overlapping) that have no wisps present (Original). The middle-panel shows the same stack but using the mock data with a wisp template added (wisp-added). The right panel shows the same stack, but applying our wisp removal algorithm to the wisp-added data (wisp-fixed). Colour scaling is per Figure 2.

means the limiting effects when increasing the image depth (with dithered exposures) is dominated by covariance and un-detected sources, and not the wisps (when using our wisp-removal process).

3. Results

The initial implementation of this processing method is written in R [8] since many of the routines necessary are provided by the PROTOOLS suite of packages written by ASGR||, and several other processing steps in the PEARLS pipeline also use this software. Basic code is provided in the Appendix, where we assume that it should be conceptually easy to re-write the procedure into any desired target language starting from this R code.

We applied the wisp-removal process to the worst-affected public PEARLS data in the NEP-TDF (PID 2738, VID 2738002001). This was done at *cal* stage 2, i.e. the output of CALWEBBIMAGE2, which is the step immediately before any more aggressive $1/f$ read-out noise removal in our pipeline. Figure 7 shows the main flow of the pipeline processing, with the original wisp-compromised image in F200W shown on the left, and the removed (middle) and final wisp template (right). Visually and statistically (in terms of the sky characteristics) we find this processing method has hugely improved the quality of the data (achieving a level similar to the tests described above).

|| <https://github.com/asgr/ProTools>

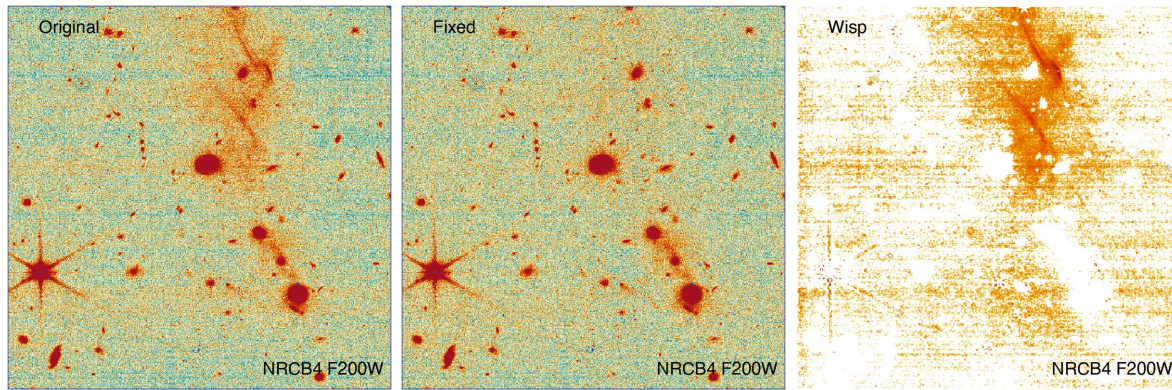


Figure 7. Example of real wisp removal. The image on the left is a F200W filter frame from NRCB4 (detector 4 of module B) taken as part of PID 2738 (VID 2738002001). The centre image shows the result of the wisp-subtracted image where the cloudy structure in the top middle of the frame has largely been removed. The right-hand image shows the wisp template that was subtracted (white pixels are the fully masked regions of the wisp that correspond to pixels we do not want to modify due to the presence of extended objects). Colour scaling is per Figure 2.

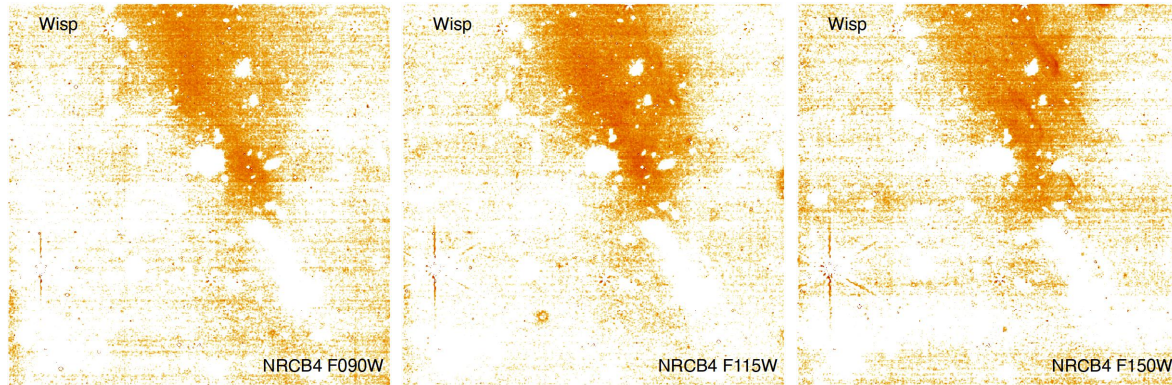


Figure 8. The same Visit ID as presented in Figure 7 but with different filters. Left image is F090W, middle image is F115W, right image is F150W. Colour scaling is per Figure 2.

3.1. Effect of Varying the Filter of the Same Detector

Universally across filters, detector NRCB4 (detector 4 of module B) is the worst affected by wisps. The wisps tend to appear in broadly the same region, but the resolution and surface brightness of the wisp varies with the filter wavelength. This can be seen in Figure 8 where we present the wisp template for the same region of sky but in different filters. F150W shows some evidence of the higher surface brightness cirrus structure in the upper right of the wisp seen clearly in Figure 7 (right panel). F090W and F115W have much more extended wisp structures, and both lack the sharper higher surface brightness diagonal features seen in F200W.

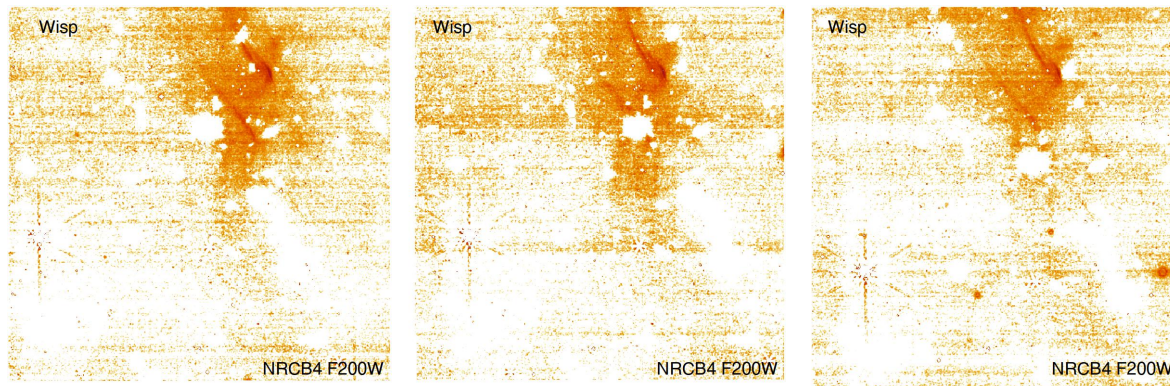


Figure 9. The same Visit ID as presented in Figure 7 and same F200W filter, but showing the three subsequent dithers within the same NRCB4 detector. Colour scaling is per Figure 2.

3.2. Effect of Small Dithers for the Same Filter and Detector

A key question is how much our wisp template varies with small dithers, i.e. when we are considering a fixed filter and the same detector. Since F200W in detector NRCB4 is the most dramatically affected by wisps, we consider small dithers of the data presented in Figure 7. Figure 9 shows the effect of such small (a few arc second) dithers. The general shape is quite consistent, but in detail it is clear the intensity of the higher and lower surface brightness parts of the wisp do vary quite notably.

3.3. Effect of the Same Filter and Varying Detectors

As discussed above, the NRCB4 is the detector most seriously affected by wisps in general. This is followed by the NRCB3 detector (where they tend to present in the bottom part of the image) and to a much lesser extent NRCA3 and NRCA4. This can be seen in Figure 10, where there is some mild wisp structure towards the bottom of NRCB3 (right panel) and much less evident structure in NRCA3 and NRCB4 (left and middle panels respectively). In this example, removing wisps from NRCA3 and NRCA4 is probably not necessary, but the method used ensures that we will, on average, correct the effect of wisps more than remove any real flux (i.e Figure 5).

4. Conclusions

In this paper we have presented a pragmatic, dynamic strategy to mitigate wisps in NIRCam short-wavelength detector data. This only relies on a good reference stack in one of the long wavelength NIRCam detectors, and *does not require the long-term construction of wisp templates*. This is significant, since it is clear after 9 months of science operations that the structure and strength of wisps is highly sensitive to the exact position and orientation of JWST. These wisps presumably have a scattered light origin, where the presence and spectrum of off-axis bright stars has a complex effect on

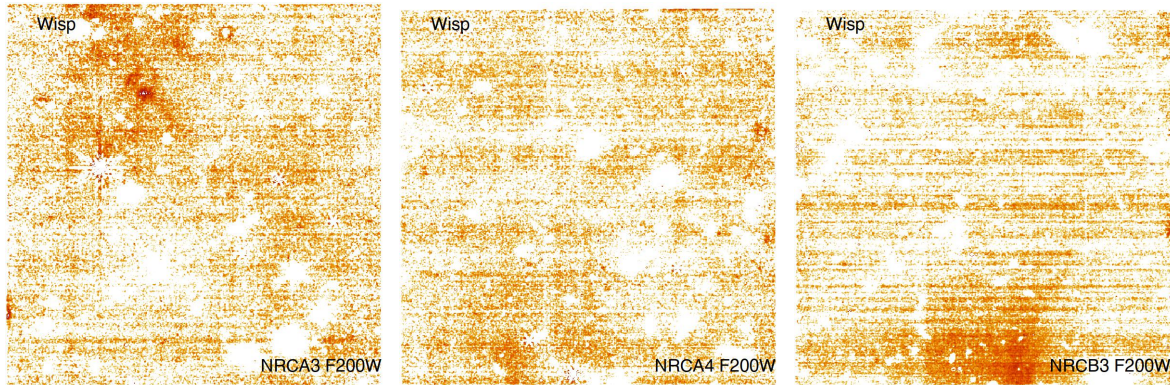


Figure 10. The same Visit ID as presented in Figure 7 and same F200W filter, but showing the NRCA3 (left), NRCA4 (middle) and NRCB3 (right) detectors, each of which is less affected by wisps than NRCB4. Colour scaling is per Figure 2.

the wisp pattern found in the raw images. Our hope is that many medium and deep surveys with JWST will benefit from incorporating a similar wisp-removal strategy, allowing survey depth to improve with \sqrt{T} throughout the image.

We include reference code written in the R programming language in the Appendix. All the functions and algorithmic steps can be easily replaced with PYTHON, IDL or JULIA equivalents.

Acknowledgements

ASGR acknowledges funding by the Australian Research Council (ARC) Future Fellowship scheme (FT200100374, ‘Hot Fuzz’). RAW and RAJ acknowledge support from NASA grants NAG5-12460, NNX14AN10G and 80NSSC18K0200 from GSFC. SPD acknowledges funding by the Australian Research Council (ARC) Laureate Fellowship scheme (FL220100191). CNAW acknowledges support from the NIRCcam Development Contract NAS5-02105 from NASA Goddard Space Flight Center to the University of Arizona.

Software: PROFOUND: <https://github.com/asgr/ProFound> [5, 9] (LGPL-3). PROPANE: <https://github.com/asgr/ProPane> (LGPL-3). RFITS: <https://github.com/asgr/Rfits> (LGPL-3). RWCS: <https://github.com/asgr/Rwcs> (LGPL-3).

References

- [1] Rieke M J, Kelly D and Horner S 2005 Overview of James Webb Space Telescope and NIRCcam’s Role *Cryogenic Optical Systems and Instruments XI (Society of Photo-Optical Instrumentation Engineers (SPIE) Conference Series vol 5904)* ed Heaney J B and Burriesci L G pp 1–8

- [2] Windhorst R A, Cohen S H, Jansen R A, Summers J, Tompkins S, Conselice C J, Driver S P, Yan H, Coe D, Frye B, Grogin N, Koekemoer A, Marshall M A, O'Brien R, Pirzkal N, Robotham A, Ryan R E, Willmer C N A, Carleton T, Diego J M, Keel W C, Porto P, Redshaw C, Scheller S, Wilkins S M, Willner S P, Zitrin A, Adams N J, Austin D, Arendt R G, Beacom J F, Bhatawdekar R A, Bradley L D, Broadhurst T, Cheng C, Civano F, Dai L, Dole H, D'Silva J C J, Duncan K J, Fazio G G, Ferrami G, Ferreira L, Finkelstein S L, Furtak L J, Gim H B, Griffiths A, Hammel H B, Harrington K C, Hathi N P, Holwerda B W, Honor R, Huang J S, Hyun M, Im M, Joshi B A, Kamieneski P S, Kelly P, Larson R L, Li J, Lim J, Ma Z, Maksym P, Manzoni G, Meena A K, Milam S N, Nonino M, Pascale M, Petric A, Pierel J D R, del Carmen Polletta M, Röttgering H J A, Rutkowski M J, Smail I, Straughn A N, Strolger L G, Swirbul A, Trussler J A A, Wang L, Welch B, B Wyithe J S, Yun M, Zackrisson E, Zhang J and Zhao X 2023 *AJ* **165** 13 (*Preprint* 2209.04119)
- [3] Finkelstein S L, Bagley M B, Ferguson H C, Wilkins S M, Kartaltepe J S, Papovich C, Yung L Y A, Arrabal Haro P, Behroozi P, Dickinson M, Kocevski D D, Koekemoer A M, Larson R L, Le Bail A, Morales A M, Pérez-González P G, Burgarella D, Davé R, Hirschmann M, Somerville R S, Wuyts S, Bromm V, Casey C M, Fontana A, Fujimoto S, Gardner J P, Giavalisco M, Grazian A, Grogin N A, Hathi N P, Hutchison T A, Jha S W, Jogee S, Kewley L J, Kirkpatrick A, Long A S, Lotz J M, Pentericci L, Pierel J D R, Pirzkal N, Ravindranath S, Ryan R E, Trump J R, Yang G, Bhatawdekar R, Bisigello L, Buat V, Calabrò A, Castellano M, Cleri N J, Cooper M C, Croton D, Daddi E, Dekel A, Elbaz D, Franco M, Gawiser E, Holwerda B W, Huertas-Company M, Jaskot A E, Leung G C K, Lucas R A, Mobasher B, Pandya V, Tacchella S, Weiner B J and Zavala J A 2023 *ApJL* **946** L13 (*Preprint* 2211.05792)
- [4] Treu T, Roberts-Borsani G, Bradac M, Brammer G, Fontana A, Henry A, Mason C, Morishita T, Pentericci L, Wang X, Acebron A, Bagley M, Bergamini P, Belfiori D, Bonchi A, Boyett K, Boutsia K, Calabró A, Caminha G B, Castellano M, Dressler A, Glazebrook K, Grillo C, Jacobs C, Jones T, Kelly P L, Leethochawalit N, Malkan M A, Marchesini D, Mascia S, Mercurio A, Merlin E, Nanayakkara T, Nonino M, Paris D, Poggianti B, Rosati P, Santini P, Scarlata C, Shipley H V, Strait V, Trenti M, Tubthong C, Vanzella E, Vulcani B and Yang L 2022 *ApJ* **935** 110 (*Preprint* 2206.07978)
- [5] Robotham A S G, Davies L J M, Driver S P, Koushan S, Taranu D S, Casura S and Liske J 2018 *MNRAS* **476** 3137–3159 (*Preprint* 1802.00937)
- [6] Windhorst R A, Carleton T, O'Brien R, Cohen S H, Carter D, Jansen R, Tompkins S, Arendt R G, Caddy S, Grogin N, Koekemoer A, MacKenty J, Casertano S, Davies L J M, Driver S P, Dwek E, Kashlinsky A, Kenyon S J, Miles N, Pirzkal N, Robotham A, Ryan R, Abate H, Andras-Letanovszky H, Berkheimer J, Chambers J, Gelb C, Goisman Z, Henningsen D, Huckabee I, Kramer D, Patel T, Pawnikar R, Pringle

- E, Rogers C, Sherman S, Swirbul A and Webber K 2022 *AJ* **164** 141 (*Preprint* 2205.06214)
- [7] Rigby J, Perrin M, McElwain M, Kimble R, Friedman S, Lallo M, Doyon R, Feinberg L, Ferruit P, Glasse A and et al 2023 *pasp* **135** 048001 (*Preprint* 2207.05632)
- [8] R Core Team 2021 *R: A Language and Environment for Statistical Computing* R Foundation for Statistical Computing Vienna, Austria URL <https://www.R-project.org/>
- [9] Robotham A S G 2018 ProFound: Source Extraction and Application to Modern Survey Data Astrophysics Source Code Library, record ascl:1804.006 (*Preprint* 1804.006)

Appendix A. R Code Implementation

Below is a compact example of our wisp removal scheme written in R. Note you will need the PROFOUND, PROPANE, RFITS and RWCS packages also (all available on GitHub at user *asgr*).

```
library(ProFound)
library(ProPane)
library(Rfits)
library(Rwcs)

wisp_im = Rfits_read_image('wisp_im.fits') #Read FITS file
ref_im = Rfits_read_image('ref_im.fits') #Read FITS file

wisp_fix = wispFixer(wisp_im, ref_im) #Run wisp removal function

Rfits_write_image(wisp_fix, 'wisp_fix.fits') #Write FITS file

#Where wispFixer is the following function:
wispFixer = function(wisp_im, #Rfits short filter image with wisps
                    ref_im, #Rfits long filter reference image
                    source_threshold = 0.95, #Threshold on reference image
                    scale_threshold = 0.95, #Quantile to define blue things
                    clip_threshold = 0.997, #Avoid very bright pixels
                    sigma = 2 #Wisp smoothing kernel
){
#Note: wisp_im and ref_im are assumed to be background subtracted

#Warp ref_im to match wisp_im WCS:
  ref_im_warp = propaneWarp(ref_im, header_out=wisp_im$header)
#Select the pixel threshold of real sources:
```

```

    real_source = quantile(ref_im_warp$imDat, source_threshold, na.rm=TRUE)
#Note, na.rm=TRUE means 'NA' flagged pixels are ignored

#Create ratio image
    relflux = (wisp_im$imDat / ref_im_warp$imDat)
#Find real sources
    relflux = relflux[ref_im_warp$imDat > real_source]
#Only consider positive relative fluxes
    relflux = relflux[relflux > 0] #ignore negative values
#Define very blue (but real) pixels
    scale = quantile(relflux, scale_threshold, na.rm=TRUE)

#Subtract scaled reference image
    wisp_template = wisp_im$imDat - ref_im_warp$imDat*scale
#Smooth the template
    wisp_template = profoundImBlur(wisp_template, sigma=sigma)
#Mask pixels we do not want to consider
    wisp_template[is.na(wisp_im$imDat) | is.na(ref_im_warp$imDat)] = NA
    wisp_template[wisp_template < 0] = NA
    wisp_template[wisp_template > quantile(wisp_template[ cont...
        wisp_template > 0], clip_threshold, na.rm=TRUE)] = NA

#Find real valued wisp template pixels
    sel = which(!is.na(wisp_template))
#Subtract from the image we wish to fix
    wisp_im$imDat[sel] = wisp_im$imDat[sel] - wisp_template[sel]

#Return the wisp corrected image
    return(wisp_im)
}

```